Published in final edited form as:
Cell Rep. 2014 March 27; 6(6): 1085–1095. doi:10.1016/j.celrep.2014.02.014.

Autocrine Effects of Tumor-Derived Complement

Min Soon Cho[1], **Hernan G. Vasquez**[1], **Rajesha Rupaimoole**[2], **Sunila Pradeep**[2], **Sherry Wu**[2], **Behrouz Zand**[2], **Hee-Dong Han**[2], **Cristian Rodriguez-Aguayo**[3], **Justin Bottsford-Miller**[2], **Jie Huang**[2], **Takahito Miyake**[2], **Hyun-Jin Choi**[2], **Heather J. Dalton**[2], **Cristina Ivan**[2], **Keith Baggerly**[3], **Gabriel Lopez-Berestein**[4,5,6], **Anil K. Sood**[2,5,6,*], and **Vahid Afshar-Kharghan**[1,*]

[1]Department of Benign Hematology, University of Texas M.D. Anderson Cancer Center, Houston, TX 77030, USA

[2]Department of Gynecologic Oncology and Reproductive Medicine, University of Texas M.D. Anderson Cancer Center, Houston, TX 77030, USA

[3]Department of Bioinformatics and Computational Biology, University of Texas M.D. Anderson Cancer Center, Houston, TX 77030, USA

[4]Department of Experimental Therapeutics, University of Texas M.D. Anderson Cancer Center, Houston, TX 77030, USA

[5]Department of Cancer Biology, University of Texas M.D. Anderson Cancer Center, Houston, TX 77030, USA

[6]Center for RNAi and Non-Coding RNA, University of Texas M.D. Anderson Cancer Center, Houston, TX 77030, USA

SUMMARY

We describe a role for the complement system in enhancing cancer growth. Cancer cells secrete complement proteins that stimulate tumor growth upon activation. Complement promotes tumor growth via a direct autocrine effect that is partially independent of tumor-infiltrating cytotoxic T cells. Activated C5aR and C3aR signal through the PI3K/AKT pathway in cancer cells, and silencing the *PI3K* or *AKT* gene in cancer cells eliminates the progrowth effects of C5aR and C3aR stimulation. In patients with ovarian or lung cancer, higher tumoral C3 or C5aR mRNA levels were associated with decreased overall survival. These data identify a role for tumor-derived complement proteins in promoting tumor growth, and they therefore have substantial clinical and therapeutic implications.

*Correspondence: asood@mdanderson.org (A.K.S.), vakharghan@mdanderson.org (V.A.-K.).

SUPPLEMENTAL INFORMATION

Supplemental Information includes six figures and one table and can be found with this article online at http://dx.doi.org/10.1016/j.celrep.2014.02.014.

INTRODUCTION

Complement proteins in plasma are mainly synthesized in hepatocytes, but endothelial cells, white blood cells, and epithelial cells also secrete complement proteins (Peng et al., 2008; Pratt et al., 2002; Raedler et al., 2009; Strainic et al., 2008). There are three pathways to activate the complement system: the *classical*, *alternative*, and *lectin* pathways. The initial steps in complement activation pathways are different, but all of them result in deposition of C3 degradation products on target surfaces and generation of anaphylatoxins (C3a and C5a) and membrane attack complex (MAC; C5b-9). Complement activation on the surface of pathogens in the blood stream helps to eradicate them from circulation. In extravascular tissues, complement proteins also participate in cell-to-cell communications and are involved in organ regeneration, angiogenesis, epithelial-mesenchymal transition, and cell migration. Despite the presence of an extensive range of responses to complement activation in normal tissues, the effect of complement activation in neoplastic tissue is not well understood. Here, we have identified a role for complement, whereby tumor-derived C3 enhances tumor growth via an autocrine pathway.

RESULTS

Biological Effects of Tumor-Derived C3 in Ovarian Cancer Cells

To address the question of whether host-derived complement proteins affect tumor growth, we first used a syngeneic mouse model of ovarian cancer in which ID8-VEGF murine ovarian cancer cells were injected into the peritoneal cavity of wild-type (WT) or C3-deficient ($C3^{-/-}$) B6 mice. After 6 weeks, there was no difference in the growth of implanted tumors between the two groups of mice (average tumor weight of 0.5 g in WT versus 0.53 g in $C3^{-/-}$ mice, n = 7 in each group; p = 0.84, t test) (Figure 1A). Surprisingly, C3 immunostaining of tumor specimens showed comparable C3 deposition in tumors resected from WT and $C3^{-/-}$ mice (Figure 1B). Because $C3^{-/-}$ mice do not produce C3, we investigated whether C3 was being produced by cancer cells. We examined a large panel of ovarian cancer cell lines for C3 mRNA levels using quantitative real-time PCR. C3 mRNA was present in all murine and in 30% of human (h) ovarian cancer cell lines (Figure 1C). To determine whether C3 is secreted by cancer cells, we measured C3 concentration in cell culture media of ovarian cancer cell lines. Supernatant of serum-free media incubated for 72 hr with normal murine ovarian endothelial cells (MOEC), murine (ID8, ID8-VEGF, and IG10), or human (SKOV3) ovarian cancer cell lines was collected and used to determine the concentration of C3 by ELISA. Ovarian cancer cells secrete much more C3 into cell culture media than control MOECs (70 ng/ml for MOECs, 4,504 ng/ml for SKOV3ip1, 332 ng/ml for ID8, 2,411 ng/ml for ID8-VEGF, and 1,329 ng/ml for IG10, Figure S1A). To determine the effects of C3 secreted by the cancer cells on the growth of implanted ovarian tumors, we reduced production of C3 in cancer cells by small interfering RNA for C3 (C3 siRNA). We used hC3 siRNAs on SKOV3ip1 ovarian cancer cells that reduced C3 mRNA and protein level by >99% (Figures S1B and S1C). Next, we examined whether C3 knockdown would have direct effects on tumor cell proliferation, migration, and invasion (Figure 1D). C3 silencing in SKOV3ip1 reduced the proliferation rate at the 48 hr time point by 55%, migration at 6 hr by 84%, and invasive potential at 24 hr by 78% compared to cancer cells

transfected with scrambled siRNA. The effects of C3 silencing on migration and invasion were measured using short-term assays and were likely to be independent of the effects on proliferation.

C3 Silencing in Ovarian Cancer Cells Reduces Tumor Growth In Vivo

To evaluate the in vivo effects of C3 knockdown on tumor growth, we used hC3 siRNA in tumor-bearing mice. We selected the most efficient hC3 siRNA in vitro (Figure S1B), conjugated it with 1,2-dioleoyl-sn-glycero-3-phosphatidylcholine (DOPC) nano-liposomes, and injected it into the peritoneal cavity of SKOV3ip1 tumor-bearing mice twice per week for 4 weeks starting 1 week after injection of cancer cells. Control mice underwent the same procedures except that they received scrambled siRNA-DOPC. The hC3 siRNA did not affect murine C3 mRNA level in mouse ovarian cancer cells in vitro and did not decrease plasma C3 levels in mice (Figures S1D and S1F). Mice receiving hC3 siRNA had about 70% reduction in their tumor burden after 4 weeks in comparison to mice receiving scrambled siRNA (average tumor weight of 0.19 g in C3 siRNA versus 0.61 g in scrambled siRNA, n = 10 mice/group; p = 0.017; Figure 1E). The number of tumor nodules was also significantly lower in mice injected with hC3 siRNA than controls (4.4 in C3 siRNA versus 11.4 in scrambled siRNA; p = 0.05; Figure 1E). Treatment with hC3 siRNA decreased C3 expression in vivo as determined by immunostaining of resected tumors (Figure 1F). C3 silencing reduced the proliferation index from 70% to 40% in tumors harvested at the end of this experiment (Figure 1G). Moreover, microvessel density (number of CD31+ lumens per high-power field) in tumors was also reduced by >50% after C3 silencing in cancer cells (Figure 1G). Although tumor-associated endothelial cells originate from the murine host and should not be affected by hC3 siRNA, we investigated whether reduction in tumor growth might be due to an inhibitory effect of hC3 siRNA on endothelial cell proliferation. We transfected the immortalized human vesicular endothelial cell line, RF24, with hC3 siRNA or scrambled siRNA and after 48 hr measured the proliferation rate using 5-ethynil-2′-deoxyuridine (EdU) incorporation assay. C3 knockdown did not reduce the proliferation rate of RF24 cells (n = 3; p = 0.07, t test; Figure 1H). We tested a second human ovarian cancer cell line (OVCAR 5) in the murine model of ovarian cancer and observed a similar reduction in tumor growth (average tumor weight of 0.27 g in C3 siRNA versus 0.63 g in scrambled siRNA, n = 10 mice/group; p = 0.02; Figures S2A and S2B).

To study the possibility of an off-target effect of C3 siRNA in cancer cells, we used ovarian cancer cells with low C3 expression (HeyA8) to induce tumor in mice, and we further manipulated expression of C3 in induced tumors using C3 siRNA and compared the growth of tumors in these mice to those tumors induced by the same cell line in mice treated with scrambled control siRNA (n = 5 in each group). The size of tumor induced by C3-low HeyA8 cells was similar in mice injected with C3 siRNA (1.402 g) or control scrambled siRNA (1.472 g) (p = 0.9; Figure S2C), showing that C3 siRNA did not affect the growth of tumor induced by C3-low cells.

C5 Silencing in Ovarian Cancer Cells Reduces Tumor Growth In Vivo

C3 activation is upstream to several other steps in the common complement pathway, such as activation of C5, release of C5a, and formation of C5b-9. To identify whether the effect

of C3 on cancer cells depends on complement activation, we used hC5 siRNA to knock down C5 gene expression in cancer cells (Figure S1G) and investigated its effect on tumor growth. C5 gene knockdown, similar to C3 silencing, reduced proliferation, migration, and invasion of SKOV3ip1 cells in vitro (Figure 2A) by 66%, 60%, and 60%, respectively, as compared to the scrambled siRNA group. In vivo, C5 silencing reduced tumor growth and proliferation index in tumor-bearing mice (average tumor weight of 0.19 g in C5 siRNA versus 0.41 g in scrambled siRNA, n = 10 mice/group; ≤0.05, t test) (Figures 2B and 2D). Reduction of C5 protein in vivo was confirmed by immunostaining tumors resected from mice treated with C5 siRNA (Figure 2C). The presence of a similar consequence for C3 and C5 knockdown in cancer cells pointed to the involvement of the complement activation pathway, rather than C3 alone, in promoting tumor growth. To confirm activation of the complement system in the tumor microenvironment, we investigated the presence of complement activation end products in tumor. MAC (C5b-9) is generated upon complement activation and inserted into the membrane of target cells. We studied the presence of C5b-9 in tumors resected from patients and tumor-bearing mice by immunostaining using C9 monoclonal antibody and antibody against C5b-9 neoepitope. In all tumor specimens, cancer cells were strongly positive for C5b-9 (Figures S3A and S3B). Interestingly, tumor stroma was negative for C5b-9 stain, confirming that cancer cells are the main target of complement activation. We also measured production of C3a, another complement activation product, in the cell culture media of cancer cells. Although serum-free media had 0.033 ng/ml of C3a, supernatant of media collected after 48 hr incubation with scrambled siRNA-transfected SKOV3ip1 cells had 3.77 ng/ml of C3a that increased to 19.7 ng/ml after 7 days. On the other hand, media incubated with SKOV3ip1 cells transfected with C3 siRNA had 2.1 and 0.7 ng/ml of C3a after 48 hr and 7 days, respectively (Figure S3C). These results confirmed that C3a is generated in the cell culture media and is originated from C3 secreted from cancer cells. To confirm that complement proteins involved in the complement activation inside the tumor are originated locally, we immunostained tumors resected from tumor-bearing $C3^{-/-}$ and WT mice using antibody to C5b-9 (Figure S3D). Tumors induced by murine ovarian cancer cells (ID8-VEGF) stained positively for C5b-9 in both $C3^{-/-}$ and WT mice.

Complement Effects on Tumor Growth Are Independent of T Cells

Next, we studied whether complement activation promotes tumor growth via a direct autocrine effect on cancer cells or through an indirect effect by altering the immune response of the host to the tumor. To study the effect of complement proteins secreted by cancer cells on the host's immune response, we carried out experiments in an immune-competent mouse model of ovarian cancer. For these experiments, we introduced C3 small hairpin RNA (shRNA) into ID8-VEGF murine ovarian cancer cells to silence the C3 gene (Figure S5A). Stably C3 shRNA-transduced ID8-VEGF cells or control cells (ID8-VEGF cells transduced with scrambled shRNA) were injected into the peritoneal cavity of $C3^{-/-}$ and WT B6 mice. C3 shRNA-transfected ID8-VEGF cells generated significantly smaller tumor nodules in both WT and $C3^{-/-}$ mice compared to control cells: in WT mice, average tumor weight of 0.77 g for scrambled shRNA-expressing cells and 0.06 g for C3 shRNA-expressing cells, n = 10 mice/group (p = 0.0001); in $C3^{-/-}$ mice, average tumor weight 0.60 g in scrambled shRNA-expressing cells and 0.03 g in C3 shRNA-expressing cells, n = 10

mice/group ($p = 0.0001$) (Figure 3A). Interestingly, reduction of C3 in tumor cells resulted in an increase of more than 10-fold in the number of CD8+ cytotoxic T cells infiltrating the tumor and an 80% reduction in the number of CD11b+ myeloid cells in tumors (Figures 3B and 3C).

To investigate whether a reduction in the number of tumor-infiltrating cytotoxic CD8+ cells determines the progrowth effect of complement on tumor, we compared tumor growth in *CD8*$^{-/-}$ and WT mice. Silencing of the C3 gene by C3 shRNA in ID8-VEGF cancer cells prior to intraperitoneal injection reduced the size and number of tumor nodules in *CD8*$^{-/-}$ and WT mice to the same magnitude (Figures 3D and 3E). There was no significant difference in the size or number of tumor nodules induced by scrambled shRNA-transduced ID8-VEGF cells between WT and *CD8*$^{-/-}$ mice. We concluded that the increase in the number of tumor-infiltrating cytotoxic CD8+ cells after C3 silencing in cancer cells observed in the immune-competent host is not responsible for the decrease in tumor growth.

Role of Anaphylatoxin Receptors in Cancer Cells

To confirm the presence of autocrine stimulation of cancer cells as a result of complement activation, we studied the effect of complement activation end products (anaphylatoxins) on cancer cells by incubating SKOV3ip1 human ovarian cancer cells with agonist peptides to C5aR and C3aR or to scrambled peptide (Langer et al., 2010). The reason for using agonist peptides to C5aR and C3aR rather than C5a and C3a is that anaphylatoxins (C3a and C5a) are extremely labile molecules and rapidly degrade to much less-potent C3a-des arg and C5a-des arg. SKOV3ip1 cells (as well as A2780, HeyA8, and OVCAR5) and murine ovarian cancer cells (ID8, ID8-VEGF, IG10, and 3B11) express anaphylatoxin receptors (Figures S4A–S4D). Exposure to 0.1 μM C5aR and C3aR agonist peptides for 48 hr increased proliferation (25% and 37%, respectively), migration (10% and 29%, respectively), and invasion (30% and 100%, respectively) in SKOV3ip1 cells (Figure 4A) compared to scrambled peptide-exposed cells ($n = 3$ in triplicates; $p < 0.01$, t test). On the other hand, C5aR and C3aR inhibitors reduced proliferation of SKOV3ip1 cells about 20% ($n = 3$; $p \leq 0.001$) (Figure 4B). We also used complement-inhibiting peptide, Compstatin (150 μg/ml), to inhibit cleavage of C3 by C3 convertase. Compstatin reduced the proliferation rate in SKOV3 cells by 15% (Figure 4C).

To further investigate the role of anaphylatoxin receptors in cancer cells, we generated stably transduced murine ovarian cancer cells (ID8-VEGF) using C3aR shRNA, C5aR shRNA, C5L2 shRNA, and scrambled shRNA (Figures S5A and S5B). We compared the weight of tumor induced by these cells in WT B6 mice. Knockdown of C5L2 in ID8-VEGF cells did not affect tumor growth, but C3aR and C5aR knockdown, similar to C3 knockdown, significantly reduced the size of induced tumors compared to control mice injected with scrambled shRNA-transduced ID8-VEGF cells (Figures S5C and S5D).

Anaphylatoxin receptors are G protein-coupled receptors and might signal through the phosphatidylinositol 3-kinase (PI3K)/ AKT pathway (Dorsam and Gutkind, 2007; Perianayagam et al., 2002). We investigated the effect of C3aR and C5aR agonist peptides on the PI3K/AKT signaling pathway in ovarian cancer cells and detected an increase in AKT mRNA (Figure 4D) and enhanced phosphorylation of p85 (a regulatory subunit of

PI3K) and AKT as a result of stimulation of C3aR and C5aR (Figure 4E). Immunostaining of tumor tissues for phosphorylated AKT (p-AKT S473) showed a reduction in p-AKT as a result of C3 silencing (Figure 4F). Silencing of PI3K or AKT by relevant siRNAs eliminated the C5aR agonist- and C3aR agonist-induced enhanced proliferation of SKOV3ip1 cells. Silencing of PI3K or AKT without exposure to C3aR and C5aR agonists did not diminish, but increased, proliferation in SKOV3ip1 cells (Figure 4G). From these results, we concluded that anaphylatoxins enhance tumor growth through the PI3K/AKT signaling pathway.

Clinical Relevance of Tumoral C3 and C5aR Expression in Ovarian Cancer

To correlate our findings in cell lines and mice to the behavior of ovarian cancer in humans, we quantified the amount of C3 mRNA in tumor specimens obtained from 75 patients with ovarian cancer. The baseline clinical and pathologic characteristics of these patients are summarized in Table S1. Patients with a higher expression of C3 mRNA in their tumor had significantly shorter overall survival (OS) compared to those with low-C3 mRNA-expressing tumors (mean OS of 36 versus 82.8 months for low versus high C3, respectively; $p = 0.004$) (Figure 4H). Expression levels of C5aR in ovarian tumors also affected the OS of 562 patients with ovarian cancer in The Cancer Genome Atlas (TCGA), with shorter average OS (40.4 months) for patients with a higher expression of C5aR and longer survival (51.3 months) for patient with a lower level of C5aR in their tumors (Figure 4I) ($p = 0.019$).

A General Role for Complement in Cancer Growth

To investigate whether complement proteins could be produced by other cancer cells besides ovarian cancer, we analyzed expression of C3 mRNA in different cancer cell lines using the Cancer Cell Line Encyclopedia (CCLE) database (http://www.broadinstitute.org/ccle/home) and identified a high level of C3 expression in liver, kidney, lung, endometrium, and ovarian cancer cell lines (Figure S6A). To evaluate the functional effects of complement protein expression in these cancer cell lines, we identified uterine (Hec265) and lung squamous cell (H226) cancer cell lines with a high expression level of C3 (Figure 5A) and reduced expression of C3, C5, and C5aR in these cells using appropriate siRNAs. Similar to the findings with ovarian cancer cells, reduction of C3, C5, or C5aR was associated with a reduction in the proliferation rate of uterine and lung cancer cells in vitro (Figures 5B and 5C). We also examined tumoral expression of complement proteins in other cancers besides ovarian cancer using TCGA database and identified a high tumoral expression of C3 in lung, uterine, and kidney cancers (Figure S6B). Among these, we examined the correlation between expression of C5aR mRNA in lung cancer specimens and survival rate. There was a significant correlation between OS and tumor expression of C5aR among 167 patients with lung cancer, with an average OS of 34.8 months for patients with a high expression level of C5aR in their tumors and 98.0 months for those with a low expression level of C5aR ($p = 0.026$) (Figure 4J).

DISCUSSION

We provide evidence that complement production and activation in tumor microenvironment enhance tumor growth by a direct autocrine effect. A few studies have

revealed a progrowth effect of complement in cancer (Corrales et al., 2012; Gunn et al., 2012; Rutkowski et al., 2010b), in which the systemic level of complement proteins had an indirect effect on cancer growth via altering the immune response of host to the tumor. Our findings provide a paradigm in which local tumoral production and activation of complement were found to be distinctly important for promoting tumor growth. The systemic production of complement by liver did not affect cancer as was evident by a similar growth of implanted tumors in $C3^{-/-}$ and WT mice and by deposition of complement activation end products in resected tumors from $C3^{-/-}$ mice. The importance of complement proteins in the cell-cell interactions has previously been shown in the antigen-presenting cells (APCs) and T cell cognate complexes in the T cell/APC interface, where complement proteins secreted by APCs regulate T cell proliferation and differentiation (Kemper and, Atkinson 2007; Longhi et al., 2006; Peng et al., 2008; Sacks, 2010; Strainic et al., 2008).

We found that complement production by cancer cells altered immune cells infiltrating into tumors (increased myeloid-derived suppressor cells and reduced cytotoxic T cells), consistent with what is described by Markiewski et al. (2008); however, in our study, the effect of complement on tumor growth was not dependent on the number of cytotoxic T cells, and silencing of C3 in cancer cells reduced tumor growth in $CD8^{-/-}$ mice to the same extent as that in WT mice. For that reason, we focused our attention on a direct effect of complement activation on tumor growth rather than on an indirect immunomodulatory effect. Our results showed an autocrine effect of complement proteins secreted by cancer cells on tumor growth (Figure 6) mediated by a direct effect of complement activation on cancer cells: (1) we found that C5b-9 complexes are deposited on cancer cells in tumors resected from patients and tumor-bearing mice, sparing other stromal cells; (2) knockdown of C3 in endothelial cells did not affect proliferation of endothelial cells; and (3) knockdown of C3aR and C5aR in cancer cells reduced the size of induced tumors in mice. Receptors for anaphylatoxins, C3aR and C5aR, are G protein-coupled receptors present on many cell types, including activated lymphocytes, monocytes, neutrophils, and epithelial cells. Activation of C5aR results in a variety of responses, including antiapoptotic responses in neutrophils (Perianayagam et al., 2002, 2004) and T cells (Lalli et al., 2008) and increase in cell proliferation in endothelial (Kurihara et al., 2010) and colon cancer cell lines (Cao et al., 2012). We showed that C5aR and C3aR agonists increased proliferation, migration, and invasion of ovarian cancer cells, and C5aR and C3aR antagonists decreased proliferation of these cells. Anaphylatoxin receptors signal through the PI3K/AKT pathway in cancer cells, and the proliferative effect of C5aR and C3aR stimulation could be eliminated by AKT silencing. Although here we link anaphylatoxins to tumor growth, these results are not completely unexpected, considering that anaphylatoxins (C3a and C5a) and sublytic concentration of C5b-9 can activate mitogenic signaling pathways, activate cell cycle, upregulate expression of growth factor genes (hepatocyte growth factor, platelet-derived growth factor, and basic fibroblast growth factor), and increase tumorigenic cytokines (interleukin-6, tumor necrosis factor α, and transforming growth factor β) (Rutkowski et al., 2010a).

In summary, we have identified a prominent role for tumor-derived complement production and activation in ovarian cancer growth and progression. These data provide a new

understanding of the role of complement in cancer biology and have significant implications for innovative therapeutic and biomarker strategies for ovarian and other cancers (Brodsky et al., 2008; Hill et al., 2010; Hillmen et al., 2006).

EXPERIMENTAL PROCEDURES

Reagents

All cell lines were obtained from ATCC. h ovarian cancer cell lines (HeyA8, SKOV3ip1, A2780, A2774, OVCAR3, OVCAR5, OVCAR8, and IGROV) were maintained in RPMI 1640 with 15% heat-inactivated fetal bovine serum (FBS) supplemented with 0.1% gentamycin sulfate (Gemini Bio-Products). h endometrial cancer cell lines (SK-UT2, Hec1A, Hec 265, Ishikawa, Spec2, and AN3CA) were maintained in Dulbecco's modified Eagle's medium (DMEM), RPMI 1640, or minimal essential medium (MEM) with 10% heat-inactivated FBS supplemented with 0.1% gentamycin sulfate. h lung cancer cell lines (HOP-92, H1299, and H226) were maintained in MEM with 10% heat-inactivated FBS supplemented with 0.1% gentamycin sulfate. Murine ovarian cell lines (ID8, ID8-VEGF, IG10, 1C5, 1F5, 3B11, 2C12, and 2C6) were maintained in DMEM with 5% heat-inactivated FBS supplemented with 0.1% gentamycin sulfate. RNA was extracted from various cancer cell lines using the RNeasy Plus Kit (QIAGEN) or TRIzol (Invitrogen) following the manufacturer's protocol. All in vitro experiments were conducted using 60%–80% confluent cell cultures. Female athymic NU/NU mice were purchased from Taconic and WT C57BL/6, *C3*$^{-/-}$, and *CD8*$^{-/-}$ mice from The Jackson Laboratory. Mice were cared for in accordance with guidelines set forth by the American Association for Accreditation of Laboratory Animal Care and the US Public Health Service Policy on Human Care and Use of Laboratory Animals. Rabbit anti-mouse C3 antibody (Abgent), mouse anti-hC3 antibody (Acris Antibodies), rabbit anti-hC5 antibody (Abcam), rabbit polyclonal anti-Ki67 antibody (Thermo Scientific/Lab Vision), rat anti-mouse CD31 antibody (BD Biosciences, BD PharMingen), mouse anti-C5b-9 antibody (Dako), mouse anti-C9 antibody (Hycult Biotech), anti-CD8 and anti-CD11b antibodies (AbD Serotec), rabbit-anti-h AKT, p-AKT, P85, and p-P85 antibodies (Cell Signaling Technology), C5aR antagonist (W-54011) (Sumichika et al., 2002):N-((4-dimethylami-nophenyl)methyl)-7-methoxy-1,2,3,4-tetrahydronaphthalen-1-carboxamide, HCl, and C3aR antagonist (SB290157) (Ames et al., 2001):N2-((2,2-diphenylethoxy)acetyl)-L-arginine (EMD Chemicals), 3,3′-diaminobenzidine (DAB; Open Biosystems), and Gill's #3 hematoxylin (Sigma-Aldrich) were purchased from the perspective commercial sources. Primer and siRNA sequences are available upon request.

Murine Model of Ovarian Cancer

All of the studies on mice were conducted according to the protocols approved by the institutional review board and Institutional Animal Care and Use Committee of the University of Texas M.D. Anderson Cancer Center (UT MDACC). Orthotopic murine models of ovarian cancer were generated by intraperitoneal injection of cancer cells. In the athymic nude model, 1×10^6 human ovarian cancer cells were resuspended in 200 μl of Hank's balanced salt solution and injected into the peritoneum of NU/NU mice. In the syngeneic immune-competent model, the same number of murine ovarian cancer cells was injected intraperitoneally to C57BL/6 WT, *C3*$^{-/-}$, or *CD8*$^{-/-}$ mice. In both models, 4–6

weeks after injection, mice became moribund and were sacrificed. Tumor nodules were resected from peritoneum, counted, and weighed. Some tumor nodules were fixed in formalin, and others were saved as fresh frozen samples by embedding in optimum cutting temperature (O.C.T.) compound. In some experiments, siRNAs conjugated to DOPC-based liposomes were injected to the tumor-bearing mice at a dose of 150 μg/kg/mouse twice a week for 4–6 weeks starting 1 week after injection of cancer cells.

Immunostaining

Immunohistochemical analyses for C3, C5, C5b-9, C9, and Ki67 were performed on 4-μm-thick formalin-fixed paraffin-embedded epithelial cancer specimens. Slides were deparaffinized with xylene and decreasing concentrations of ethanol and rehydrated with PBS. Antigen retrieval was performed using 1× Borg-decloaker (dilute 1:10 in distilled water if 10×) (BioCare Medical) under steamer cooker at 65°C for 45 min followed by 80 min cooldown at room temperature. Endogenous peroxidases were blocked with 3% hydrogen peroxide in PBS followed by washes with PBS. Nonspecific binding was blocked with 5% normal horse serum and 1% normal goat serum in PBS for 20 min. Immunohistochemical analyses for CD31, CD8, and CD11b were performed on 4 μm O.C.T. compound-embedded fresh frozen cancer specimens. Slides were fixed with acetone and acetone:chloroform and rehydrated with PBS. Nonspecific binding was blocked with 5% normal horse serum in PBS for 20 min. Primary antibodies (C3, C5, C5b-9, C9, Ki67, CD8, CD11b, pAKT, and CD31) were diluted to 1:200 concentration using 5% normal horse serum (100–200 μl/slide) and incubated overnight at 4°C. After washing, biotinylated secondary antibodies were incubated for 20 min and amplified using the streptavidin horseradish peroxidase label (4plus Mouse-on-Mouse Avidin-Biotin Detection; BioCare Medical) for 20 min. After washing with PBS, the slides were incubated with 100–200 μl of DAB at room temperature, counterstained with hematoxylin for 15 s, and mounted on a bright-field microscope.

Immunofluorescence Staining

ID8-VEGF tumor cells were stably transduced with murine C3 shRNA, C3aR shRNA, C5aR shRNA, or C5L2 shRNA carrying lentiviri and plated at a density of 5×10^3 cells in a 2-well chamber slide. Twenty-four hours after plating, tumor cells were fixed with 4% paraformaldehyde for 30 min and permeabilized in 0.01% Triton X-100 in PBS for 10 min. Following incubation with the primary antibodies (C3, C3aR, C5aR, and C5L2, 1:100 diluted in 1% BSA-PBS) for 1 hr at room temperature, cells were incubated with the secondary antibodies (goat anti-rabbit Alexa 594, 1:1,000 diluted; chicken anti-goat Alexa 594, 1:1,000 diluted) (Life Technologies) for 1 hr at room temperature. DAPI (Life Technologies) was used as a nuclear counterstain. Images were obtained using the Zeiss Axioplan 2 Fluorescence microscope.

Quantitative Real-Time PCR

Total RNA was prepared from h or murine ovarian cancer cell lines using the RNeasy Plus Kit. cDNA was synthesized from 1 μg of total RNA using the Thermo Scientific Verso cDNA Synthesis Kit according to the manufacturer's protocol, followed by quantitative real-time PCR using the ABsolute Blue QPRC Low ROX Mix (Thermo Scientific) and primers

for h or murine C3, C5, C3aR, and C5aR mRNAs. The sequences of primers are available upon request.

Cell Proliferation Analysis

Cell proliferation was measured by incorporation of fluorescence-conjugated EdU to the newly synthesized DNA, according to the manufacturer's protocol (Click-iT EdU Alexa Fluor; Invitrogen). Briefly, ovarian cancer cells were plated at a density of 5×10^4 cells in a 6-well dish and transfected with siRNAs. Forty-eight hours after transfection, tumor cells were treated with 10 mM EdU for 2 hr, washed three times with PBS, detached with 0.25% EDTA, fixed with 4% paraformaldehyde for 15 min, immunostained with anti-EdU-FITC (1:200), and analyzed using flow cytometry (EPICS XL 4-Color Cytometer; Beckman Coulter).

Mouse Plasma C3 ELISA

The concentration of C3 in serum samples was determined using mouse C3 ELISA kit, according to the manufacturer protocol (GenWay Biotech). Blood samples for this assay were collected from mice before tumor dissection, and the plasma C3 concentration was determined using a calibration curve constructed with different dilutions of mouse C3.

ELISAs on Cell Culture Media

The concentration of C3 and C3a in cell culture media from SKOV3ip1 cells was determined using hC3 ELISA kit (GenWay Biotech) and C3a ELISA Plus Kit (Quidel), respectively, according to the manufacturer protocol. Culture media samples for this assay were collected from serum-free media at indicated time points, and secreted C3 and C3a concentrations in culture media were determined using a calibration curve constructed with different dilution of hC3 and hC3a.

Invasion and Migration Assays

We used modified Boyden chambers (Coster) coated with either defined matrix (invasion) or 0.1% gelatin (migration). Untreated cells (8×10^4 cells for migration and 4×10^4 cells for invasion) were suspended in 500 μl serum-free media and added into the upper chamber. Complete media containing 10% FBS (500 μl) were added to the bottom chamber as a chemoattractant. The chambers were incubated at 37°C in 5% CO_2 for either 6 hr (migration) or 24 hr (invasion). After incubation, the cells in the upper chamber were removed with cotton swabs. Migrating or invading cells to the bottom chamber were fixed, stained, and counted by light microscopy from five random fields.

siRNA Delivery

For in vitro transfections, cancer cells were incubated with a siRNA/liposome mixture with a ratio of 2 μg siRNA to 3 μl of liposome suspension (Lipofectamine reagent; Life Technologies) for 48 hr. Prior to transfection, cells were incubated in serum-free media for 24 hr. For in vivo delivery, siRNAs were incorporated into DOPC-based liposomes. Briefly, siRNAs were mixed with DOPC in the presence of excess tertiary butanol (1:10 w/w siRNA/DOPC), then mixed with Tween 20 (1:19 v/v Tween 20/siRNA-DOPC), and finally

lyophilized and stored at −80°C until use. Immediately prior to in vivo administration, the lyophilized preparation was hydrated with 0.9% saline.

Preparation of shRNA and Stable Cell Lines

Murine C3 shRNA, C3aR shRNA, C5aR shRNA, and C5L2 shRNA carrying lentiviri were produced by the core facility for molecular cloning and lentivirus production system in the Department of Cancer Biology at UT MDACC. Briefly, murine C3 shRNA, C3aR shRNA, C5aR shRNA, C5L2 shRNA, or scrambled sequence was cloned into pGreenPuro lentiviral vectors (pGreenPuro; System Biosciences) and tagged with GFP. A total of 20 μg of these cloned lentiviral vectors was transfected into HEK293T cells along with 15 μg of packaging plasmid (2nd generation psPAX2; Addgene) and 15 μg of envelope plasmid (2nd generation pMD2G) using FuGENE transfection reagent (Promega) in accordance with the manufacturer's protocol. Supernatants containing the lentivirus were collected, filtered, and added to the cancer cells in the presence of 8 μg/ml Polybrene (Promega). Twenty-four hours later, 4 μg/ml of puromycin was added to the media for 7 days. Transduction efficiency of the cells was calculated by dividing the number of GFP-expressing cells by the total number of cells and was found to be 100% in all of the experiments. Transduced cells were analyzed by quantitative real-time PCR assay to determine the level of C3 mRNA silencing.

Tumor Samples and Clinical Data from Patients with Cancer

All of the studies on the h subjects were conducted according to the approved protocol of the institutional review board of the UT MDACC. We obtained tumor samples from 75 patients with invasive epithelial ovarian cancer from specimens stored in the M.D. Anderson Cancer Center's Tumor Bank (Merritt et al., 2008). Clinical data relevant to these patients were obtained from patients' medical records. Using quantitative real-time PCR, we compared and normalized ovarian cancer patients' C3 mRNA expression level to an average of six normal individuals' C3 mRNA expression. TCGA data portal (http://tcga.cancer.gov) was used to download information on clinically annotated information on patients with high-grade serous ovarian cancer and squamous cell lung cancer. The OS duration was defined as the interval (in months) between the date of initial surgical resection to death or last follow-up. For TCGA database analysis, we randomly split the entire population into training/validation cohorts (2/3 and 1/3), and we checked for a relation with survival. Using the training set, we identified the optimal cutoff of approximately 0.3, which was then validated in a separate cohort. Access to TCGA database was approved by the National Cancer Institute. The UT MDACC approved the waiver for performing this survival analysis with deidentified database information.

Statistical Analysis

In the experiments with animal models of ovarian cancer, the null hypothesis of no difference in tumor weights and number of tumor nodules between each experimental group and control was tested against the alternative hypothesis that the experimental treatment reduced tumor weights or number of nodules. Based on our preliminary data, we estimated that the coefficient of variation to be 0.65 for changes in tumor weight and 0.75 for changes in the number of tumor nodules. For an effect size (ratio of fixed effect and residual SD) of

0.65, a sample size of n = 10 mice in each group was sufficient to provide 80% power for a test at significance level of 0.05.

Tumor weights and the number of tumors in each mouse group were compared using the Student's t test or the Mann-Whitney U rank sum test. Two-tailed p values of less than 0.05 were deemed statistically significant. Continuous variables with normal distribution were compared using the Student's t test, and those that were not normally distributed were compared using a nonparametric test (Mann-Whitney U test). Only two-tailed values are reported in this study. Statistical analysis of the clinical data was performed using two-sample t test and Fisher's exact test. Survival analysis was performed using Kaplan- Meier analysis.

Supplementary Material

Refer to Web version on PubMed Central for supplementary material.

Acknowledgments

We would like to thank Donna Reynolds and Robert Langley for their guidance with immunohistochemistry studies. B.Z., J.B.-M., and H.j.C. were supported by an NIH T32 Training Grant CA101642. This work was also supported in part by NIH grants (P50CA083639, CA109298, P50CA098258, P30CA016672, UH2TR000943, U54CA151668, U54CA96300, U54CA96297, and R01CA177909), CPRIT RP110595, Ovarian Cancer Research Fund Program Project Development Grant, Department of Defense (OC073399, OC120547, and OC100237), the Zarrow Foundation, the Betty Ann Asche Murray Distinguished Professorship, the Marcus Foundation, the RGK Foundation, the Gilder Foundation, and the Blanton-Davis Ovarian Cancer Research Program.

References

Ames RS, Lee D, Foley JJ, Jurewicz AJ, Tornetta MA, Bautsch W, Settmacher B, Klos A, Erhard KF, Cousins RD, et al. Identification of a selective nonpeptide antagonist of the anaphylatoxin C3a receptor that demonstrates antiinflammatory activity in animal models. J Immunol. 2001; 166:6341–6348. [PubMed: 11342658]

Brodsky RA, Young NS, Antonioli E, Risitano AM, Schrezenmeier H, Schubert J, Gaya A, Coyle L, de Castro C, Fu CL, et al. Multi-center phase 3 study of the complement inhibitor eculizumab for the treatment of patients with paroxysmal nocturnal hemoglobinuria. Blood. 2008; 111:1840–1847. [PubMed: 18055865]

Cao Q, McIsaac SM, Stadnyk AW. Human colonic epithelial cells detect and respond to C5a via apically expressed C5aR through the ERK pathway. Am J Physiol Cell Physiol. 2012; 302:C1731–C1740. [PubMed: 22496247]

Corrales L, Ajona D, Rafail S, Lasarte JJ, Riezu-Boj JI, Lambris JD, Rouzaut A, Pajares MJ, Montuenga LM, Pio R. Anaphylatoxin C5a creates a favorable microenvironment for lung cancer progression. J Immunol. 2012; 189:4674–4683. [PubMed: 23028051]

Dorsam RT, Gutkind JS. G-protein-coupled receptors and cancer. Nat Rev Cancer. 2007; 7:79–94. [PubMed: 17251915]

Gunn L, Ding C, Liu M, Ma Y, Qi C, Cai Y, Hu X, Aggarwal D, Zhang HG, Yan J. Opposing roles for complement component C5a in tumor progression and the tumor microenvironment. J Immunol. 2012; 189:2985–2994. [PubMed: 22914051]

Hill A, Rother RP, Wang X, Morris SM Jr, Quinn-Senger K, Kelly R, Richards SJ, Bessler M, Bell L, Hillmen P, Gladwin MT. Effect of eculizumab on haemolysis-associated nitric oxide depletion, dyspnoea, and measures of pulmonary hypertension in patients with paroxysmal nocturnal haemoglobinuria. Br J Haematol. 2010; 149:414–425. [PubMed: 20230403]

Hillmen P, Young NS, Schubert J, Brodsky RA, Socié G, Muus P, Röth A, Szer J, Elebute MO, Nakamura R, et al. The complement inhibitor eculizumab in paroxysmal nocturnal hemoglobinuria. N Engl J Med. 2006; 355:1233–1243. [PubMed: 16990386]

Kemper C, Atkinson JP. T-cell regulation: with complements from innate immunity. Nat Rev Immunol. 2007; 7:9–18. [PubMed: 17170757]

Kurihara R, Yamaoka K, Sawamukai N, Shimajiri S, Oshita K, Yukawa S, Tokunaga M, Iwata S, Saito K, Chiba K, Tanaka Y. C5a promotes migration, proliferation, and vessel formation in endothelial cells. Inflamm Res. 2010; 59:659–666. [PubMed: 20217457]

Lalli PN, Strainic MG, Yang M, Lin F, Medof ME, Heeger PS. Locally produced C5a binds to T cell-expressed C5aR to enhance effector T-cell expansion by limiting antigen-induced apoptosis. Blood. 2008; 112:1759–1766. [PubMed: 18567839]

Langer HF, Chung KJ, Orlova VV, Choi EY, Kaul S, Kruhlak MJ, Alat-satianos M, DeAngelis RA, Roche PA, Magotti P, et al. Complement-mediated inhibition of neovascularization reveals a point of convergence between innate immunity and angiogenesis. Blood. 2010; 116:4395–4403. [PubMed: 20625009]

Longhi MP, Harris CL, Morgan BP, Gallimore A. Holding T cells in check—a new role for complement regulators? Trends Immunol. 2006; 27:102–108. [PubMed: 16406700]

Markiewski MM, DeAngelis RA, Benencia F, Ricklin-Lichtsteiner SK, Koutoulaki A, Gerard C, Coukos G, Lambris JD. Modulation of the antitumor immune response by complement. Nat Immunol. 2008; 9:1225–1235. [PubMed: 18820683]

Merritt WM, Lin YG, Han LY, Kamat AA, Spannuth WA, Schmandt R, Urbauer D, Pennacchio LA, Cheng JF, Nick AM, et al. Dicer, Drosha, and outcomes in patients with ovarian cancer. N Engl J Med. 2008; 359:2641–2650. [PubMed: 19092150]

Peng Q, Li K, Anderson K, Farrar CA, Lu B, Smith RA, Sacks SH, Zhou W. Local production and activation of complement up-regulates the allostimulatory function of dendritic cells through C3a-C3aR interaction. Blood. 2008; 111:2452–2461. [PubMed: 18056835]

Perianayagam MC, Balakrishnan VS, King AJ, Pereira BJ, Jaber BL. C5a delays apoptosis of human neutrophils by a phosphatidylinositol 3-kinase-signaling pathway. Kidney Int. 2002; 61:456–463. [PubMed: 11849385]

Perianayagam MC, Balakrishnan VS, Pereira BJ, Jaber BL. C5a delays apoptosis of human neutrophils via an extracellular signal-regulated kinase and Bad-mediated signalling pathway. Eur J Clin Invest. 2004; 34:50–56. [PubMed: 14984438]

Pratt JR, Basheer SA, Sacks SH. Local synthesis of complement component C3 regulates acute renal transplant rejection. Nat Med. 2002; 8:582–587. [PubMed: 12042808]

Raedler H, Yang M, Lalli PN, Medof ME, Heeger PS. Primed CD8(+) T-cell responses to allogeneic endothelial cells are controlled by local complement activation. Am J Transplant. 2009; 9:1784–1795. [PubMed: 19563342]

Rutkowski MJ, Sughrue ME, Kane AJ, Ahn BJ, Fang S, Parsa AT. The complement cascade as a mediator of tissue growth and regeneration. Inflamm Res. 2010a; 59:897–905. [PubMed: 20517706]

Rutkowski MJ, Sughrue ME, Kane AJ, Mills SA, Parsa AT. Cancer and the complement cascade. Mol Cancer Res. 2010b; 8:1453–1465. [PubMed: 20870736]

Sacks SH. Complement fragments C3a and C5a: the salt and pepper of the immune response. Eur J Immunol. 2010; 40:668–670. [PubMed: 20186746]

Strainic MG, Liu J, Huang D, An F, Lalli PN, Muqim N, Shapiro VS, Dubyak GR, Heeger PS, Medof ME. Locally produced complement fragments C5a and C3a provide both costimulatory and survival signals to naive CD4+ T cells. Immunity. 2008; 28:425–435. [PubMed: 18328742]

Sumichika H, Sakata K, Sato N, Takeshita S, Ishibuchi S, Nakamura M, Kamahori T, Ehara S, Itoh K, Ohtsuka T, et al. Identification of a potent and orally active non-peptide C5a receptor antagonist. J Biol Chem. 2002; 277:49403–49407. [PubMed: 12384495]

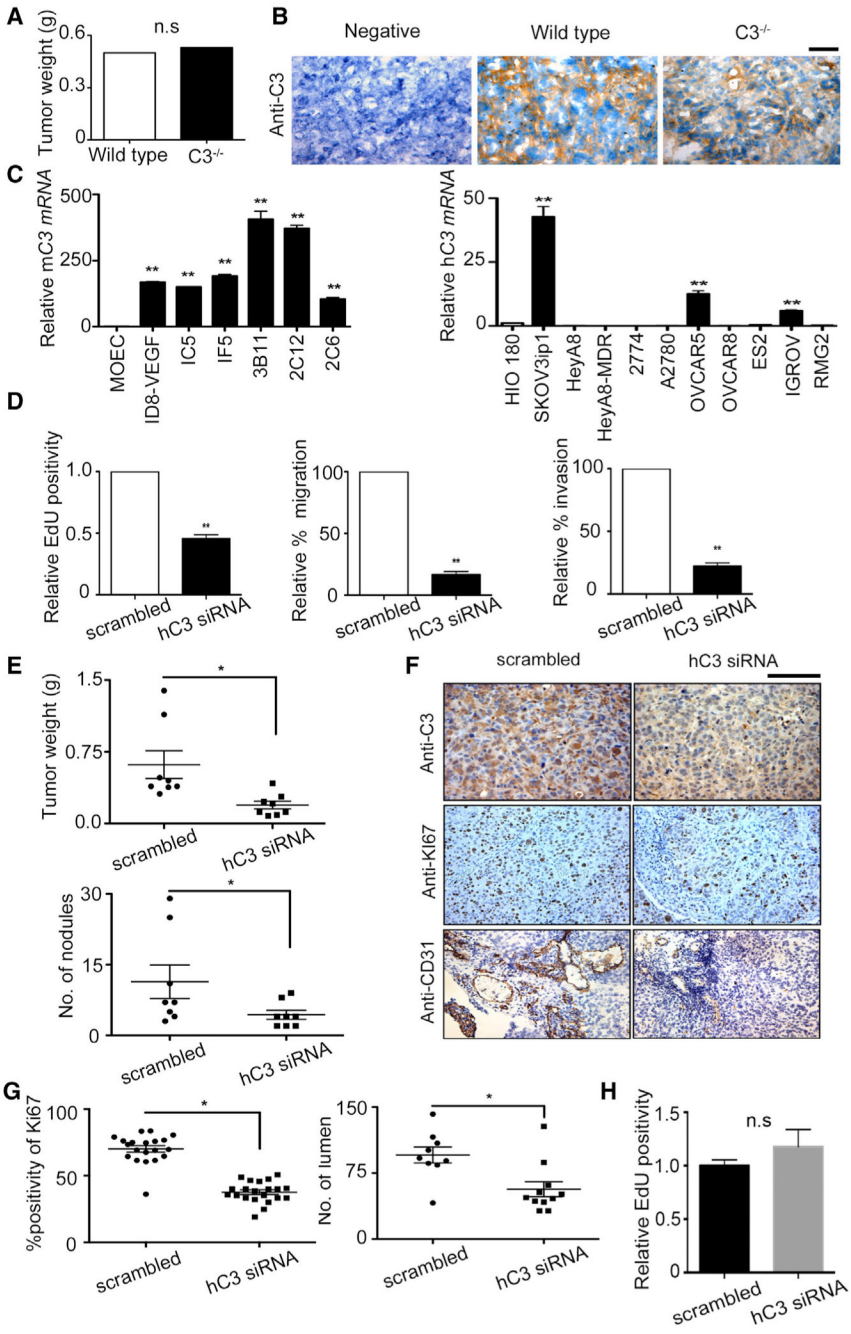

Figure 1. Ovarian Cancer Cells Secrete Complement Proteins, which Enhance Tumor Growth

(A) We measured total tumor weight in an orthotopic murine model of ovarian cancer induced by ID8-VEGF murine ovarian cancer cells in *C3*$^{-/-}$ and WT control mice, both in C57BL/6 background. n.s, not significant.

(B) Immunostaining of tumors induced by ID8-VEGF in WT and *C3*$^{-/-}$ mice, using anti-C3 antibody compared to negative control stain (secondary antibody alone). Scale bar length is 100 μm.

(C) Quantitative real-time PCR for C3 mRNA on RNA isolated from murine and human ovarian cancer cell lines. Expression of C3 mRNA in cancer cell lines was compared to that in MOECs and normal human ovarian surface epithelial cell lines (HIO 180) ($n = 3$; $^{**}p \leq 0.01$, t test).

(D) C3 gene knockdown in SKOV3ip1 human ovarian cancer cells using C3 siRNA, reduced proliferation, migration, and invasion of these cells in vitro. Results of three independent experiments (each of them in triplicate) are summarized as bar graphs ($^{**}p \leq 0.01$, t test).

(E) C3 gene knockdown in SKOV3ip1-induced tumors by intraperitoneal injection of hC3 siRNA into tumor-bearing NU/NU mice reduced total weight ($^{*}p = 0.017$) and number of tumor nodules ($^{*}p = 0.05$).

(F) Representative immunostaining for C3, Ki67, and CD31 in tumors resected from hC3 siRNA-injected and scrambled siRNA-injected mice. Scale bar, 100 μm.

(G) The proliferation index in resected tumors was quantified as the percentage of Ki67 positivity shown in dot plots (39% in C3 siRNA versus 74% in scrambled siRNA, $n = 5$ mice in each group; $^{*}p = 0.05$, t test). The number of blood vessels in resected tumors was quantified by counting the number of CD31+ lumen structures in five high-power fields (HPFs) per section and in five sections per tumor nodule and in five mice per group. Average number of CD31+ lumens per HPF is shown as dot plots (22/HPF in C3 siRNA versus 42/HPF in scrambled siRNA; $^{*}p = 0.05$, t test).

(H) We investigated the effect of complement on proliferation of endothelial cells by measuring the proliferation rate of RF24 endothelial cells after transfection with C3 siRNA. C3 knockdown did not reduce the proliferation rate in RF24 endothelial cells ($n = 3$; $p = 0.07$, t test).

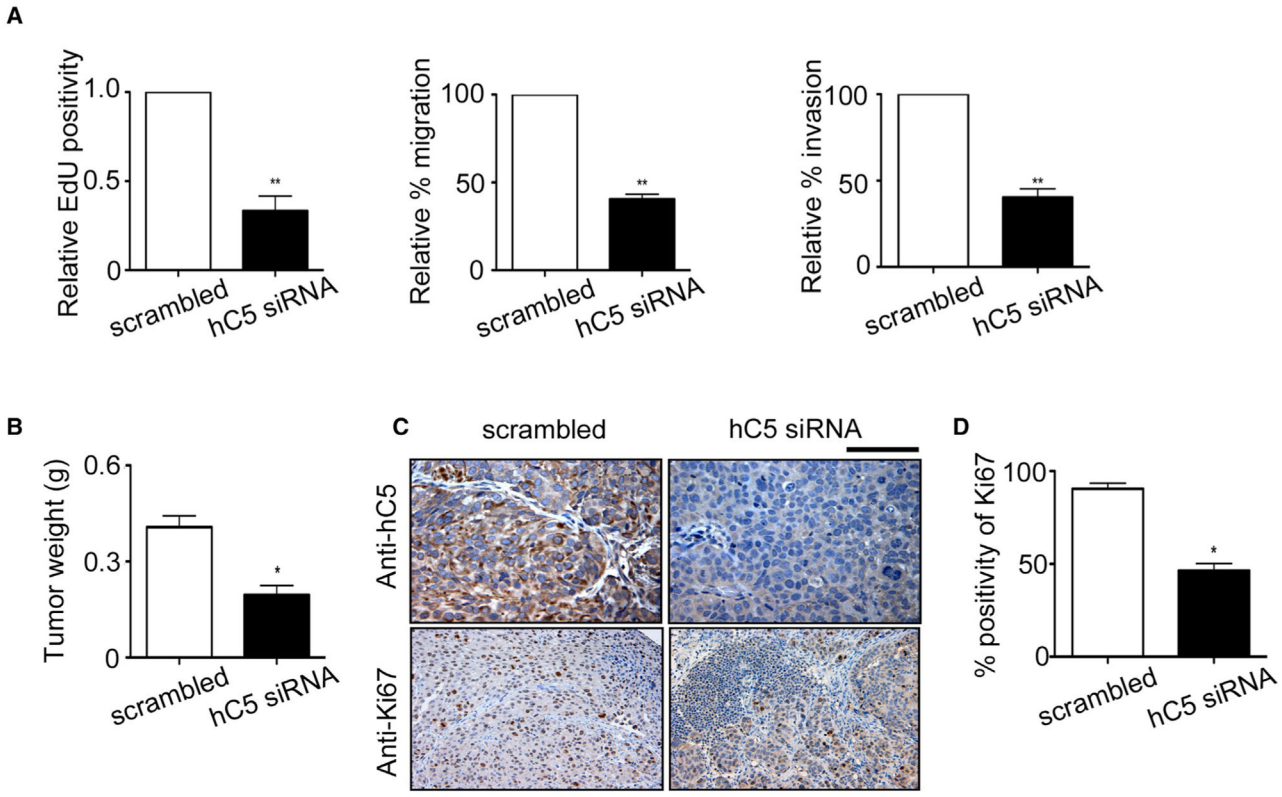

Figure 2. C5 Knockdown Decreases Tumor Growth

(A) Silencing of C5 gene expression in SKOV3ip1 cells using hC5 siRNA reduced proliferation, migration, and invasion of these cells in vitro. Results of three independent experiments (each of them in triplicate) are summarized as bar graphs (**$p \leq 0.01$, t test).

(B) C5 gene knockdown using intraperitoneal injection of hC5 siRNA into SKOV3ip1-induced tumor-bearing NU/NU mice reduced total tumor weight compared to the same mice injected with scrambled siRNA. *$p \leq 0.05$.

(C) Representative immunostaining for C5 and Ki67 in tumors resected from hC5 siRNA-injected and scrambled siRNA-injected mice. Scale bar, 100 μm.

(D) The proliferation index in resected tumors was quantified as the percentage of Ki67 positivity in bar graphs (37.1% in C5 siRNA versus 72.3% in scrambled siRNA, n = 5 in each group; *$p = 0.05$, t test).

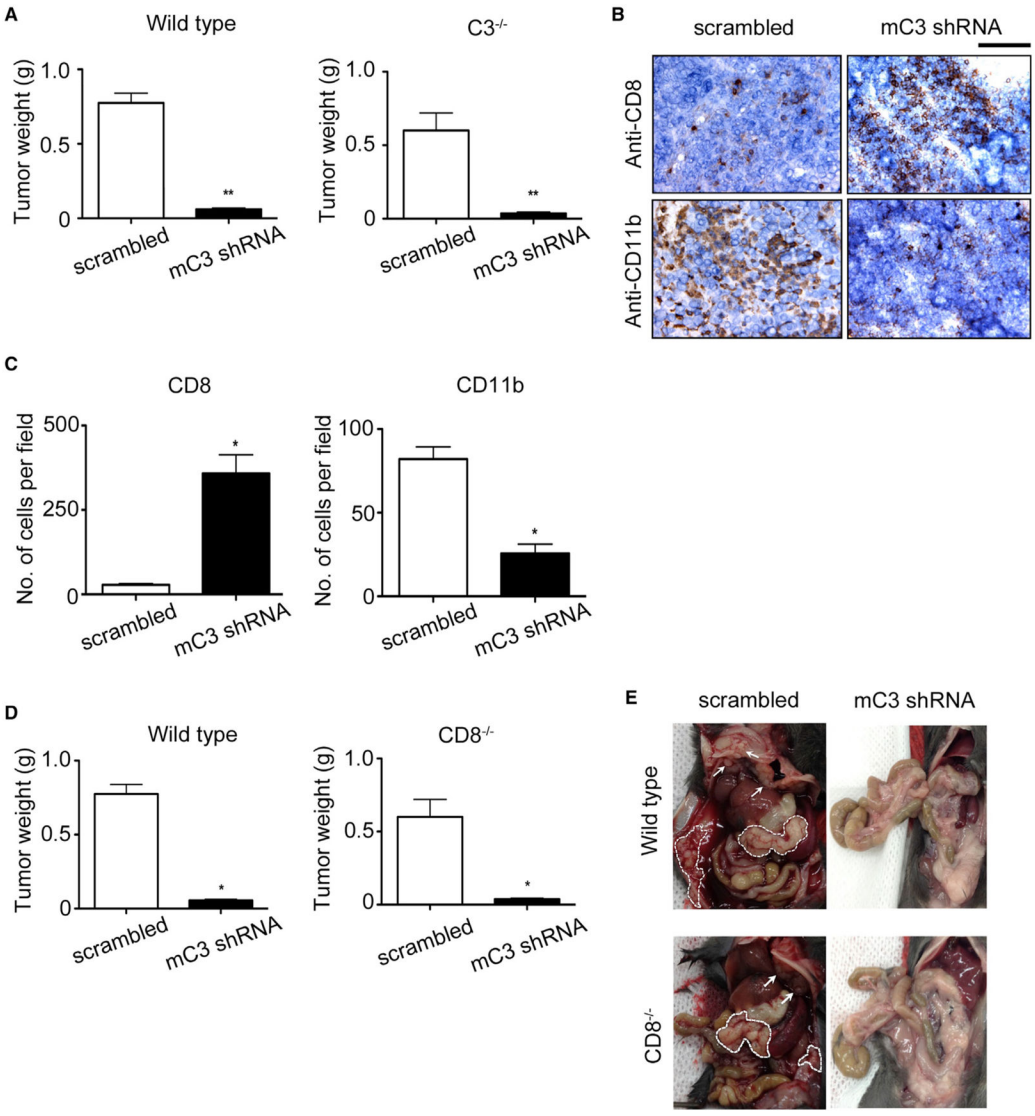

Figure 3. Role of Immunomodulatory Effect of C3 Knockdown on Tumor Growth

(A) ID8-VEGF murine ovarian cancer cells stably expressing murine (m) C3 shRNA or control scrambled shRNA were injected into immune-competent C57BL/6 mice (WT and *C3*$^{-/-}$). Cancer cells with C3 knockdown generated smaller tumors in both WT and *C3*$^{-/-}$ mice. **p ≤ 0.0001.

(B) Representative immunostaining for CD8 and CD11b in tumors induced by mC3 shRNA-expressing or scrambled shRNA-expressing ID8-VEGF cells in WT mice. Scale bar, 100 μm.

(C) The number of cytotoxic T cells (CD8+) and myeloid cells (CD11b+) were determined by counting cells in three high-power fields per tumor nodule per mouse and in five mice per group, and the results are summarized as bar graphs (28 CD8+ cells/HPF in scrambled shRNA-expressing and 358 CD8+/HPF in C3 shRNA-expressing cell-induced tumors; 82 CD11b+ cells/HPF in scrambled shRNA-expressing and average number of 25 CD11b+ cells/HPF in C3 shRNA-expressing cell-induced tumors, n = 15 HPF; *p = 0.001, t test).

(D) ID8-VEGF cells stably expressing mC3 shRNA or control scrambled shRNA were injected to *CD8*$^{-/-}$ and WT mice. There was no significant difference in tumor size after injection with scrambled shRNA-expressing cancer cells between *CD8*$^{-/-}$ and WT mice (0.60 ± 0.23 g versus 0.77 ± 0.17 g, respectively; n = 10 mice/ group; p = 0.19). C3 silencing by mC3 shRNA in cancer cells resulted in 98% reduction in tumor weight in both WT and *CD8*$^{-/-}$ mice (*p ≤ 0.001).

(E) A representative necropsy in mice showing the presence of tumor nodules on viscera and peritoneal surfaces (surrounded by dashed lines) in WT and *CD8*$^{-/-}$ mice injected with ID8-VEGF cells expressing scrambled shRNA and lack of tumor nodules in those injected with mC3 shRNA-expressing cancer cells. Arrows show tumor nodules on the peritoneal surface of diaphragm.

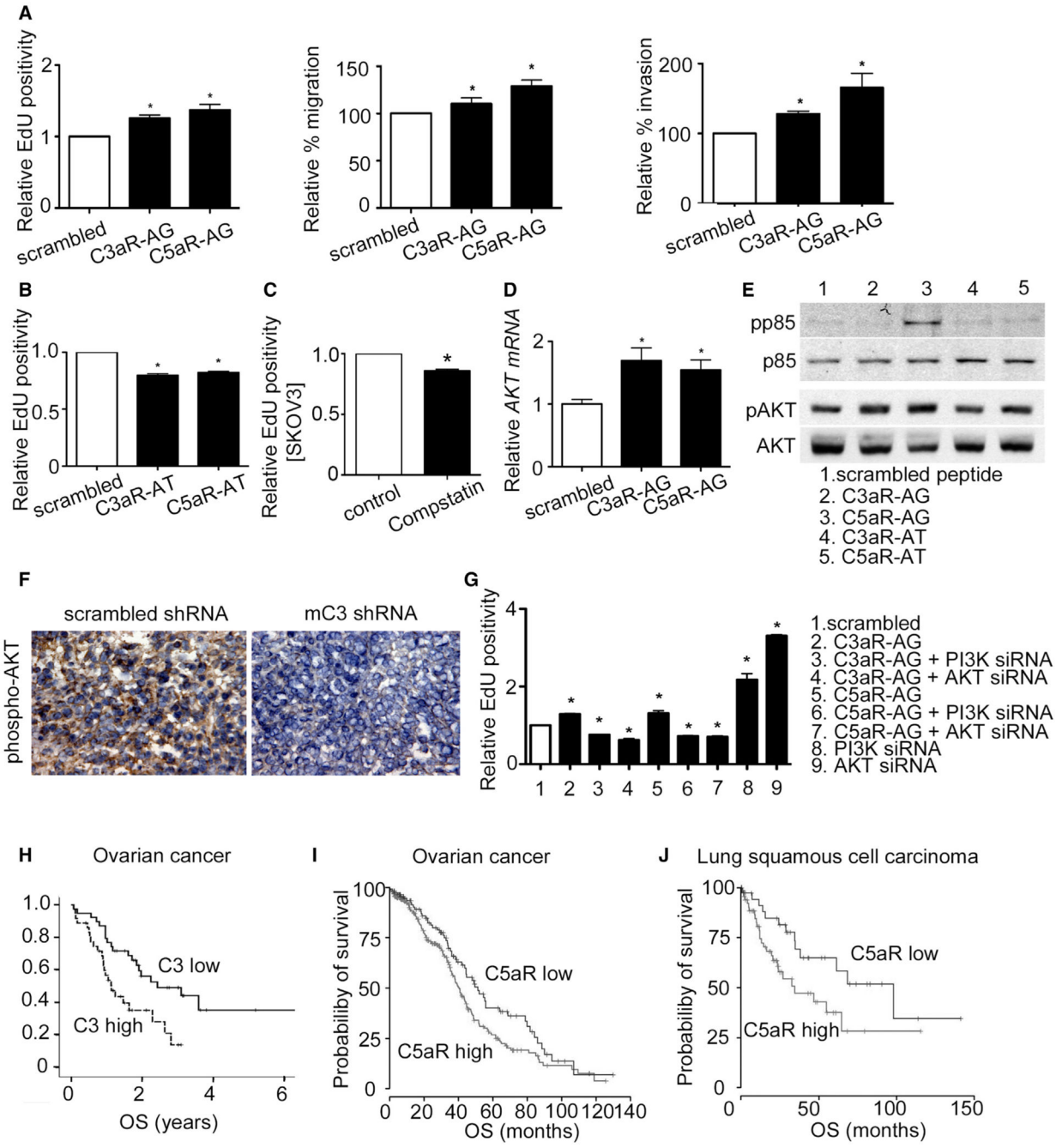

Figure 4. Direct Effect of Complement Activation on Tumor Growth

(A) Agonist peptides to anaphylatoxin receptors (C3aR-AG and C5aR-AG) increase proliferation, migration, and invasion of SKOV3ip1 human ovarian cancer cells in vitro compared to those in cells incubated with scrambled peptide (control). SKOV3ip1 cells were incubated with 0.1 μM C3aR-AG and C5aR-AG for 48 hr (proliferation),6 hr (migration),or24 hr (invasion). Results of three independentexperiments (each of them in triplicate) are summarized as bar graphs(*p ≤0.01,t test).

(B) C3aR inhibitor (W-54011), labeled as C3aR-AT, and C5aR inhibitor (SB290157), labeled as C5AR-AT, reduced proliferation of SKOV3ip1 human ovarian cancer cells in vitro compared to those in cells incubated with scrambled peptide (control). SKOV3ip1 cells were incubated with 0.1 μM C3aR-AT and C5aR-AT for 48 hr. Results of three independent experiments (each of them in triplicate) are summarized as bar graphs (*$p \leq 0.001$).
(C) SKOV3ip1 human ovarian cancer cells were incubated with Compstatin (Tocris Bioscience), a peptide inhibitor of C3 convertase, at a final concentration of 150 μg/ml or with the controlled scrambled peptide for 2 days. Cell proliferation was measured at the end of the incubation period using EdU incorporation assay. Compstatin reduced the proliferation rate in SKOV3ip1 cells by 15% ($n = 3$; *$p \leq 0.002$, t test).

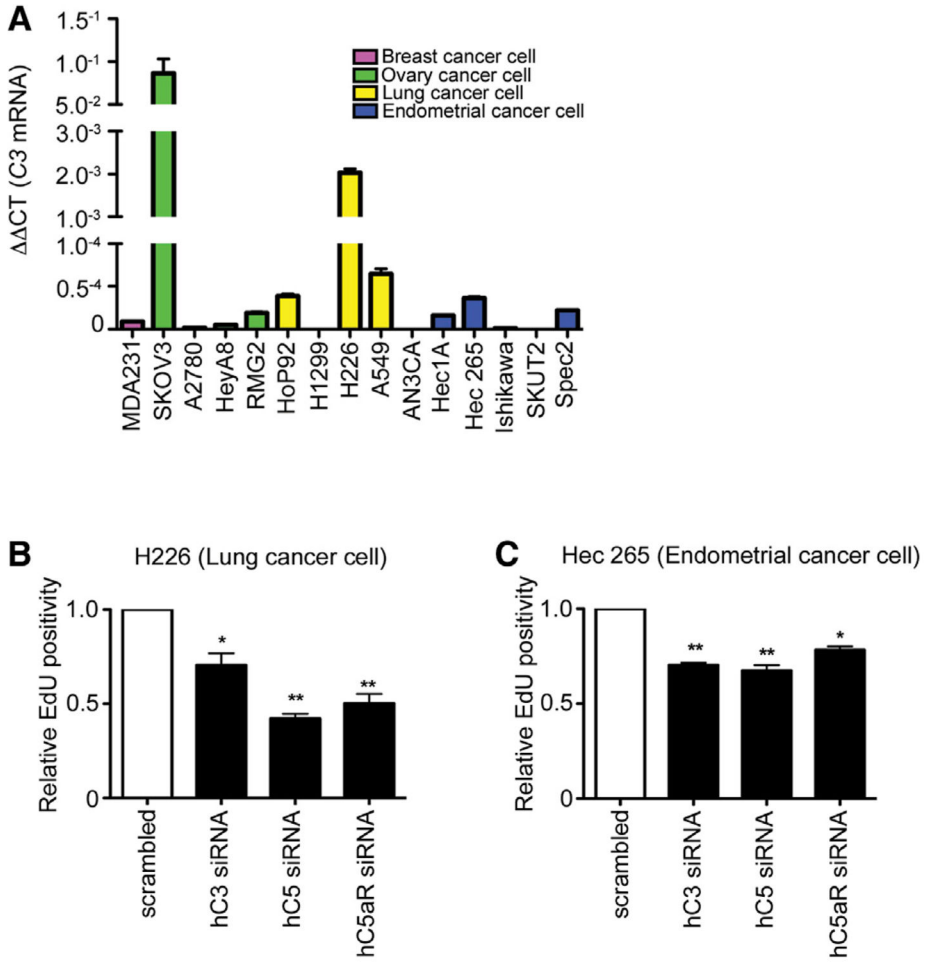

Figure 5. Cancer Cells Originated from Different Organs Secrete Complement Proteins that Enhance Cell Proliferation

(A) Quantification of C3 mRNA in h breast, ovarian, lung, and endometrium cancer cell lines using quantitative real-time PCR (n = 3).

(B and C) Reducing C3 gene expression in (B) H226 human squamous cell lung cancer and in (C) Hec265 human endometrium cancer cell lines using C3 siRNA reduced proliferation, migration, and invasion of these cells in vitro. Results of three independent experiments (each of them in triplicate) are summarized as bar graphs (*p ≤ 0.01 and **p ≤ 0.001, t test).

(D) The relative abundance of AKT mRNA in total mRNA isolated from SKOV3ip1 cells after 24 hr exposure to C3aR and C5aR agonists was quantified by quantitative real-time PCR, and the result of three experiments are summarized as bar graphs (*p ≤ 0.001).

(E) A representative immunoblot on total cell lysate prepared from SKOV3ip1 cells after 48 hr exposure to C3aR and C5aR agonists and inhibitors using antibodies to p-85, AKT, and their phosphorylated forms (n = 3).

(F) Immunostaining of tumors induced by ID8-VEGF cells expressing scrambled shRNA or mC3 shRNA in C57BL/6 mice using anti-pAKT antibody.

(G) To investigate the effect of AKT or PI3K silencing on C3aR and C5aR agonist-induced enhancement of SKOV3ip1 proliferation, expression of AKT or PI3K in SKOV3ip1 was

reduced using AKT or PI3K siRNA (data not shown), and cell proliferation was quantified 48 hr after exposure to C3aR-AG and C5aR-AG and was compared to SKOV3ip1 cells transfected with scrambled siRNA ($n = 3$; $*p \leq 0.001$).

(H) C3 mRNA level in the tumor specimens of 75 patients diagnosed with ovarian cancer in MDACC was determined using quantitative real-time PCR and correlated with their OS ($p = 0.004$) and presented as Kaplan-Meier survival curve.

(I) Correlation between expression of C5aR in tumor and OS in 562 patients with ovarian cancer in TCGA database ($p = 0.019$).

(J) The amount of C5aR mRNA in tumors resected from 167 patients with a diagnosis of lung squamous cell carcinoma was quantified using quantitative real-time PCR and was correlated to the OS of these patients as documented in TCGA database. The results are shown as Kaplan-Meier survival curve ($p = 0.026$).

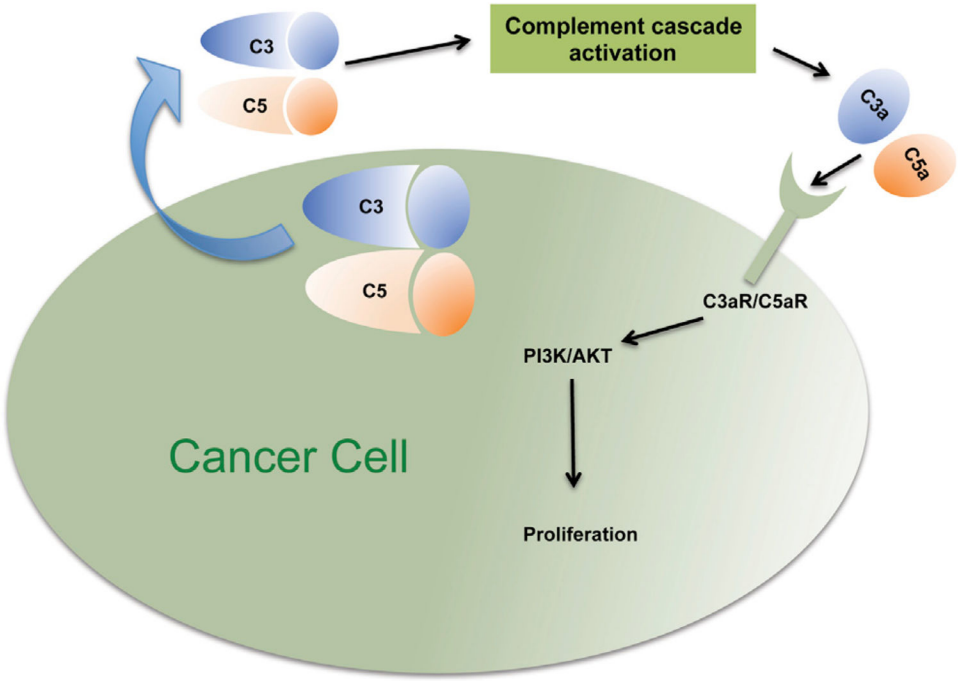

Figure 6. Cancer Cell-Produced Complement Enhances Tumor Growth in an Autocrine Manner

Cancer cells secrete complement proteins resulting in complement activation in the tumor microenvironment. Complement activation products such as C3a and C5a activate their receptors on cancer cells that through PI3K/AKT signaling increase cell proliferation.